

NASA TECHNICAL
MEMORANDUM

NASA TM X-53268

May 25, 1965

NASA TM X-53268

N65-30650

FACILITY FORM 602

(ACCESSION NUMBER)	(THRU)
<u>31</u>	<u>1</u>
(PAGES)	(CODE)
(NASA CR OR TMX OR AD NUMBER)	<u>30</u>
	(CATEGORY)

A METHOD OF IMPLEMENTING CUTOFF CONDITIONS
FOR SATURN V LUNAR MISSIONS OUT OF EARTH
PARKING ORBIT ASSUMING A CONTINUOUS GROUND
LAUNCH WINDOW

by F. DON COOPER
Aero-Astrodynamics Laboratory

NASA

*George C. Marshall
Space Flight Center,
Huntsville, Alabama*

GPO PRICE \$ _____

CFSTI PRICE(S) \$ _____

Hard copy (HC) 2.00

Microfiche (MF) .50

ff 653 July 65

TECHNICAL MEMORANDUM X-53268

A METHOD OF IMPLEMENTING CUTOFF CONDITIONS FOR SATURN V LUNAR MISSIONS
OUT OF EARTH PARKING ORBIT ASSUMING A CONTINUOUS GROUND LAUNCH WINDOW

By

F. Don Cooper

George C. Marshall Space Flight Center

Huntsville, Alabama

ABSTRACT

This report demonstrates a method of implementing cutoff conditions for the Saturn V lunar mission out of earth parking orbit assuming a ground launch window of four and one-half hours.

30650

DeBlo

NASA - GEORGE C. MARSHALL SPACE FLIGHT CENTER

Technical Memorandum X-53268

May 25, 1965

A METHOD OF IMPLEMENTING CUTOFF CONDITIONS FOR SATURN V LUNAR MISSIONS
OUT OF EARTH PARKING ORBIT ASSUMING A CONTINUOUS GROUND LAUNCH WINDOW

By

F. Don Cooper

GUIDANCE APPLICATIONS SECTION
APPLIED GUIDANCE AND FLIGHT MECHANICS BRANCH
DYNAMICS AND FLIGHT MECHANICS DIVISION
AERO-ASTRODYNAMICS LABORATORY
RESEARCH AND DEVELOPMENT OPERATIONS

TABLE OF CONTENTS

	<u>Page</u>
I. INTRODUCTION.....	1
II. GUIDANCE SCHEME AND HYPERSURFACE ERRORS.....	3
III. HYPERSURFACE ERRORS.....	4
IV. REPRESENTATION ERRORS.....	5
V. VEHICLE AND PARKING ORBIT PERTURBATIONS.....	6
VI. OPTIMUM NOMINALS.....	8
VII. CONCLUSIONS.....	9
APPENDIX I: AIM VECTOR CALCULATIONS.....	11
APPENDIX II: GUIDANCE EQUATIONS AND HYPERSURFACE.....	15
APPENDIX III: DERIVATION OF THE CUTOFF HYPERSURFACE PERIGEE EQUATION.....	23

TECHNICAL MEMORANDUM X-53268

A METHOD OF IMPLEMENTING CUTOFF CONDITIONS FOR SATURN V LUNAR MISSIONS
OUT OF EARTH PARKING ORBIT ASSUMING A CONTINUOUS GROUND LAUNCH WINDOW

SUMMARY

20650

A method of implementing Saturn V lunar missions from an earth parking orbit is presented. The ground launch window is assumed continuous over a four and one-half hour period. The iterative guidance scheme combined with a set of auxiliary equations that define suitable S-IVB cutoff conditions, is the approach taken. The four inputs to the equations that define cutoff conditions are represented as simple third-degree polynomials as a function of ignition time.

Errors at lunar arrival caused by the separate and combined effects of the guidance equations, cutoff equations and input representations are shown. Vehicle performance variations and parking orbit injection errors are included as perturbations.

Appendix I explains how aim vectors were computed for the cutoff equations. Appendix II presents all guidance equations and related implementation procedures. Appendix III gives the derivation of the auxiliary cutoff equations.

Author

No error at lunar arrival was large enough to require a midcourse correction greater than one meter per second assuming a transfer time of three days and the midcourse correction occurs five hours after injection. Since this result is insignificant when compared to expected hardware errors, the implementation procedures presented are adequate to define cutoff conditions for Saturn V lunar missions.

I. INTRODUCTION

The iterative guidance scheme will generate steering functions which will insure attainment of a desired cutoff condition. Since these steering functions are updated in flight, the cutoff condition does not have to be invariant with respect to time. Each evaluation of the guidance scheme generates steering functions which will direct the vehicle, in a near optimum maneuver, toward whatever end condition was defined for that evaluation.

A set of equations describing a cutoff condition which will satisfy a given mission is defined as a hypersurface. The hypersurface used in this report requires four basic inputs: a unit aim vector, eccentricity, cutoff energy and an aim vector magnitude. For a continuous launch capability, these four quantities are generated in the guidance computer as a function of parking orbit ignition time. The unit aim vector was implemented by fitting each component as a third-degree least square polynomial. The three magnitudes, eccentricity, cutoff energy and aim vector magnitude, were also represented as third-degree least square polynomials.

All nominal trajectories used to compute basic input data for the hypersurface were optimized for cutoff weight at lunar injection subject to three lunar end conditions: (1) radius of closest approach equal to 1923 kilometers (RCA), (2) a flight time of 72 hours from lunar injection to radius of closest approach (T_f), and (3) inclination of the flight plane with respect to the moon's equatorial plane at arrival minimized for the chosen launch time (INC). For the particular launch day selected for the error analysis, the declination of the moon at arrival was near minimum. Therefore, launch azimuth is not symmetrical with respect to launch time.

To evaluate the effectiveness of the method used to compute basic hypersurface inputs, implementation procedures, the guidance equations, and hypersurface accuracy, a set of error analyses is shown. A measure of the accuracy of any lunar injection guidance scheme is how far the nominal radius of closest approach (RCA) is missed. Each error analysis shows the RCA miss distance, time of flight variation, inclination errors and payload losses for six launch azimuths ranging from 72 to 105 degrees. This corresponds to a launch window of about 4 1/2 hours. What each error analysis shows is briefly described as follows:

- (1) Errors and performance losses caused by the guidance scheme and hypersurface.
- (2) Errors and performance losses caused by the hypersurface.
- (3) Errors and performance losses caused by the guidance scheme, hypersurface and implementation of basic hypersurface inputs by polynomial representation.
- (4) Same as (3) except vehicle performance and parking orbit perturbations are superimposed. Only a 72 degree launch azimuth case is shown, since it is representative of other azimuths.

For reference, the calculus of variations optimum nominals are shown. From these trajectories the basic hypersurface inputs were calculated as described in Appendix I.

II. GUIDANCE SCHEME AND HYPERSURFACE ERRORS

Errors at lunar arrival caused by the guidance scheme and hypersurface equations are shown in Table I. Nominal input values for the hypersurface were taken from the optimized nominal trajectories shown in Table V. Initial conditions and vehicle characteristics were the same as the optimized nominals.

TABLE I

Azimuth (deg)	Δ RCA (km)	Δ T _F (sec)	Δ INC (deg)	Δ W (lbs)
72	-3	-4	-.01	-24
77.7	2	9	.00	-25
90	-8	-13	-.01	-25
93.7	-9	-17	-.05	-25
98.4	2	8	.00	-25
105	-2	-5	.00	-24

The radius of closest approach miss distance (Δ RCA) is shown in kilometers. The deviation time of flight (Δ T_F) from the 72-hour nominal value is shown in seconds. Inclination errors (Δ INC) are usually very small, and are shown in degrees. Payload losses (Δ W), due almost entirely to the guidance scheme, are shown as the number of pounds the guided runs were below the optimized nominals whose payloads were approximately 128,000 lbs. at lunar injection. The same guidance equations which were used for ascent into an earth parking orbit were used for the lunar injection phase. Slight modification of the ascent guidance equations can reduce payload losses to about three pounds. However, since either case is acceptable, the same guidance equations are used for both operations.

Appendix II shows in detail the guidance equations, inputs required, and hypersurface equations used for these error analyses.

III. HYPERSURFACE ERRORS

Errors at lunar arrival caused by the cutoff hypersurface equations only are shown in Table II. The powered flight phase was optimized for payload by calculus of variations techniques subject to the cutoff condition specified by the hypersurface. It is emphasized that Table II does not represent guided trajectories.

TABLE II

Azimuth (deg)	Δ RCA (km)	Δ T _F (sec)	Δ INC (deg)	Δ W (lbs)
72	-3	-3	-.02	0.
77.7	-4	-2	.02	0.
90	-1	8	.16	0.
93.7	-3	4	.10	0.
98.4	-2	-1	.00	0.
105	-2	-7	.21	0.

Therefore, the deviations from the optimized nominals represent only hypersurface errors and cutoff tolerance errors. The cutoff tolerances were small enough to enforce RCA to within one kilometer and flight time within two seconds. Inclination enforcement was much more difficult to achieve, and the differences between the values shown in Table I and II show the guidance scheme can cut off in a given plane more accurately than a calculus of variations program using a reasonable number of isolation runs. Experience has shown that this is true for other types of missions as well. Payload losses were less than one pound for all cases.

IV. REPRESENTATION ERRORS

If the basic hypersurface inputs (\underline{M} , M , e , c_3) are represented as third-degree polynomials as a function of ignition time (measured from midnight), larger errors at lunar arrival will occur than if nominal hypersurface inputs are used. Table III represents guided trajectories with hypersurface inputs curve fit as a function of parking orbit ignition time. Ignition occurred when the vehicle was a fixed angle from the aim vector. Since the aim vector is a function of ignition time, a series of tests is necessary to determine ignition time. This will be no problem for the onboard computer, and the ignition criterion is satisfactory.

TABLE III

Azimuth (deg)	ΔR_{CA} (km)	ΔT_F (sec)	ΔINC (deg)	ΔW (lbs)
72	-15	9	.47	-26
77.7	30	45	1.63	-31
90	-45	-83	.29	-25
93.7	-24	-86	1.64	-30
98.4	8	-51	3.57	-40
105	-24	-56	.46	-24

After time of ignition was determined, the polynomials were evaluated and the results used as inputs to the hypersurface.

A comparison of Table III with Table I shows the radius of closest approach error increased slightly because of representation errors. The accuracy decrease is a small consideration when compared to the simplicity of implementation for an entire launch window. Larger errors are shown in this table than would be expected, because the launch window was considered to be 4 1/2 hours and the maximum allowed for a realistic mission will be 2 1/2 hours. Therefore, the nonsymmetry of the hypersurface inputs versus time resulted in larger curve-fit errors than if the more linear part of the launch window were chosen.

V. VEHICLE AND PARKING ORBIT PERTURBATIONS

Assuming the S-IVB vehicle will not perform nominally and that parking orbit injection conditions will not be perfect, Table IV presents lunar arrival errors caused by these type of perturbations for a 72-degree launch azimuth. The results are representative of any launch azimuth contained in the launch window.

TABLE IV

Perturbation	ΔR_{CA} (km)	ΔT_F (sec)	ΔINC (deg)	ΔW (lbs)
Nominal	-15	+9	.47	-26
+F	8	-23	.39	-29
-F	-47	-37	.52	-29
+I _{sp}	-24	-30	.46	-25
-I _{sp}	-16	-31	.44	-25
+W	-23	-26	.47	-25
-W	-16	-36.	.42	-25
+R	-3	-36	.41	-25
-R	-38	-25	.49	-25
+V	-16	-25	.45	-24
-V	-11	-9	.49	-27
+t _i	-37	-11	.58	-25
-t _i	12	-16	.39	-25
+t _L	-34	-70	-.04	-28
-t _L	6	32	1.84	-26

A typical S-IVB vehicle was used for the nominal case. Magnitudes of the perturbations were as follows.

$\pm F$	± 8000 lbs thrust
$\pm I_{sp}$	± 8.62 sec specific impulse
$\pm W$	± 2500 lbs weight uncertainty
$\pm R$	± 30 km parking orbit altitude variation
$\pm V$	± 15 m/sec parking orbit velocity variation
$\pm t_i$	± 15 sec time of ignition error
$\pm t_L$	± 1 minute time of launch (azimuth mis-alignment error).

These magnitudes are far larger than any expected vehicle perturbations or parking orbit variations.

If the cutoff ellipse were invariant even when a parking orbit altitude variation occurred, large payload losses would result. However, small payload losses are maintained by varying the eccentricity of the cutoff ellipse so that the altitude gain by the optimum nominal profiles is enforced. This is accomplished as a part of the cutoff hypersurface equations by computing the change in eccentricity as

$$\Delta e = \left(\frac{\partial e}{\partial r} \right) \Delta r$$

where $\partial e / \partial r$ is an analytic first order approximation. The cutoff hypersurface equations are shown in detail in the flow chart on page 16.

VI. OPTIMUM NOMINALS

The problem of computing optimum nominal lunar transfer trajectories from an earth parking orbit requires a large amount of computer time. A calculus of variations powered program assuming constant thrust and flow rate was used. Once a parking orbit is established and the lunar end conditions specified, the problem can be resolved to finding the minimum time required to transfer the vehicle from some set of initial state variables to some other set of terminal state variables subject to the lunar end conditions. The initial state variables are only a function of time of ignition. This problem can be solved in five to ten minutes on the IBM 7094 computer.

Table V shows the nominal trajectories that were used to obtain input data for the cutoff hypersurface. Small variations in RCA and flight time are caused by isolation tolerances. Time of launch is shown to illustrate the nonsymmetry of launch azimuth versus launch time. A 3-hour launch window is possible between 72 and 90 degrees launch azimuth. However, the hypersurface inputs were third-degree polynomials in time from 72 to 105 degrees launch azimuth.

TABLE V

Azimuth (deg)	RCA (km)	T _F (hr/sec)	INC (deg)	Time of Launch (hr/min)
72	1921	72/7	1.11	6/25
77.7	1922	72/5	.32	7/32
90	1922	72/3	.75	9/43
93.7	1921	72/3	.70	10/7
98.4	1923	72/13	.30	10/27
105	1922	72/3	.46	10/42

VII. CONCLUSIONS

Lunar arrival errors caused by the iterative guidance scheme, cut-off hypersurface, and representation of inputs by simple polynomials are insignificant when compared to expected errors caused by vehicle hardware. Therefore, the implementation procedures as presented are adequate to define cutoff conditions for the S-IVB vehicle.

No plane change cases have been presented. Current studies indicate that a slight modification of the hypersurface equations will increase performance for missions that require a plane change maneuver.

APPENDIX I

Aim Vector Calculation

After a nominal powered trajectory is obtained which satisfies all mission constraints, basic inputs required by the hypersurface can be computed. The basic inputs are a unit aim vector (\underline{M}), eccentricity (e), cutoff energy (c_3), and an aim vector magnitude (M). An optimum nominal trajectory is not essential. However, the set of equations that define the hypersurface will assume the cutoff condition of the nominal only when furnished the nominal range angle. Since the range angle as computed by the Iterative Guidance Scheme will be nearly optimum, if the reference is not an optimum trajectory, nominal cutoff will not occur. Therefore, it is usually desirable that the reference trajectory be an optimum so that any deviation in cutoff conditions will cause performance losses.

All trajectories used to define basic hypersurface input values were optimized for payload subject to mission constraints. No plane change maneuver was performed. Payload was optimized subject to an energy cutoff value that resulted in a desired flight time. Time of coast and time of launch were varied to meet the other constraints described in the introduction. The maximum payload possible for a given flight time was computed.

Using these optimum nominal powered flight trajectories, the basic hypersurface inputs are computed as follows with all vectors computed in the space-fixed plumbline earth-centered coordinate system.

\underline{r} = position vector at cutoff

\underline{v} = velocity vector at cutoff

r = magnitude of \underline{r}

v = magnitude of \underline{v}

$$\underline{N} = \frac{\underline{r} \times \underline{v}}{|\underline{r} \times \underline{v}|}$$

$$c_3 = v^2 - \frac{2\mu}{r} \quad \mu = .3986032 \times 10^{15} \text{ m}^3/\text{sec}^2$$

$$\sin^2 \theta = 1 - \left(\frac{\underline{r} \cdot \underline{v}}{rv} \right)^2$$

$$e = (1 + c_3 r^2 v^2 \sin^2 \theta / \mu^2)^{1/2}$$

$$a = - \frac{c_3}{\mu}$$

$$\underline{r}_p = \underline{N} \times \underline{r}$$

$$\phi_c = \arccos \left\{ \frac{1}{e} \left[\frac{a}{r} (1 - e^2) - 1 \right] \right\} .$$

After powered cutoff the vehicle coasts to the desired lunar end condition. Any point along the ballistic flight could be chosen as the aim point. For all error analyses in this report the aim point was chosen where the vehicle entered the lunar sphere of influence (defined as 35,000 statute miles from the center of the moon). The distance from the center of the earth when the vehicle entered the lunar sphere of influence was chosen as the aim vector magnitude.

M = aim vector magnitude

$$\phi_T = \arccos \left\{ \frac{1}{e} \left[\frac{a}{M} (1 - e^2) - 1 \right] \right\}$$

$$\underline{M} = \frac{1}{r} \left[\underline{r} \cos (\phi_T - \phi_c) + \underline{r}_p \sin (\phi_T - \phi_c) \right].$$

Now the four basic inputs required for the hypersurface have been computed:

\underline{M} = unit aim vector

M = aim vector magnitude

e = eccentricity

c_3 = cutoff energy.

It is important to select the aim point from an integrated ballistic flight that satisfies a desired end condition. The desired end condition need not correspond to lunar arrival conditions even though that is the final objective. For example, an aim point may be chosen where a mid-course maneuver is to occur.

Reviewing the equations used to compute the hypersurface inputs will reveal why lunar arrival errors are small when cutoff is approximated by simple elliptic equations. The desired cutoff energy and eccentricity are computed using the cutoff condition of the nominal. An arbitrary distance from the center of the earth is chosen as the aim vector magnitude. This magnitude determines the angle between the aim vector and perigee vector. Next the aim vector is computed in the nominal cutoff plane. Although the actual cutoff plane as determined by the hypersurface will depend upon parking orbit variations, the hypersurface equations will insure that the injection point defined by the hypersurface will be near the injection point of the nominal. This means that both ballistic trajectories will experience almost the same gravitational perturbations. The small differences will cause only small lunar arrival errors.

APPENDIX II
Guidance Equations and Hypersurface

A. Implementation Techniques

The guidance equations and hypersurface used for the error analysis shown in the text are presented in the form of a flow chart on page 16.

Ignition occurred when the vehicle was a fixed angle from the aim vector (TIGA was set equal to zero). This ignition criterion was used for all cases where the hypersurface inputs were represented as polynomials.

The hypersurface equations themselves can be considered the equations necessary to compute the perigee vector (\underline{S}). All other equations are used only to translate from the hypersurface coordinate system to the guidance reference system.

The guidance equations themselves begin in the block where the terminal range angle is estimated and continue until the pitch and yaw angles are computed.

In addition to the equations used to compute pitch and yaw, the computer simulation program used a pitch and yaw rate given as

$$K_2 = \frac{K_1 A_p}{B_p}$$

and

$$K_4 = \frac{K_3 A_y}{B_y},$$

respectively.

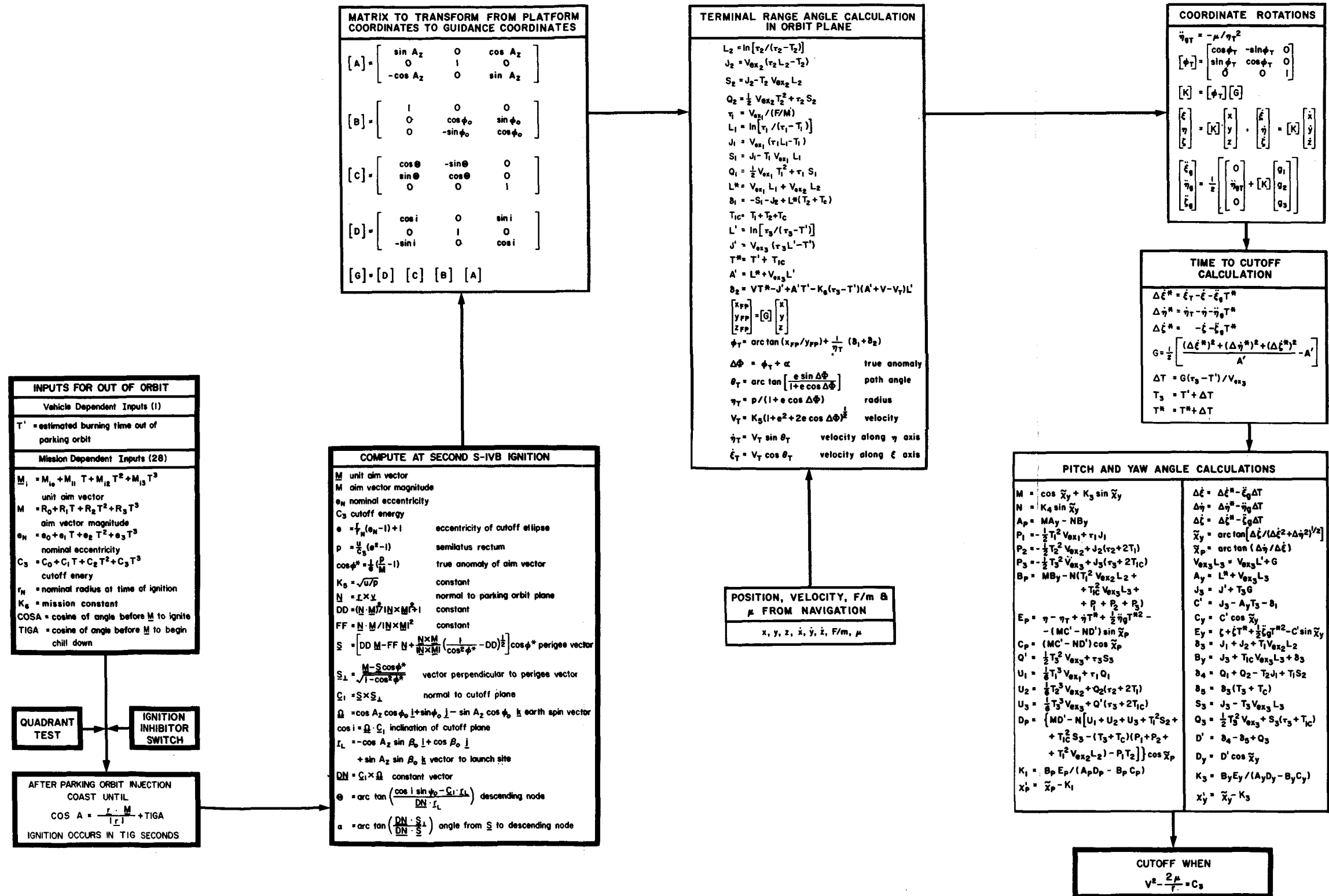
Therefore, the equations for χ_p' and χ_y' (chi pitch and chi yaw in the guidance reference coordinate system) become

$$\chi_p' = \tilde{\chi}_p - K_1 + K_2 \delta t$$

$$\chi_y' = \tilde{\chi}_y - K_3 + K_4 \delta t,$$

where small δt is defined as the time since the guidance equations were last evaluated.

ITERATIVE GUIDANCE MODE EQUATIONS FLIGHT OUT OF ORBIT



It is important to the guidance implementation procedure to fix the end conditions as predicted in the terminal range angle block about 25 seconds before cutoff. Normally K_1 , K_2 , K_3 and K_4 are frozen 10 seconds before cutoff. This procedure prevents large turning rates from building up after the guidance parameters are frozen.

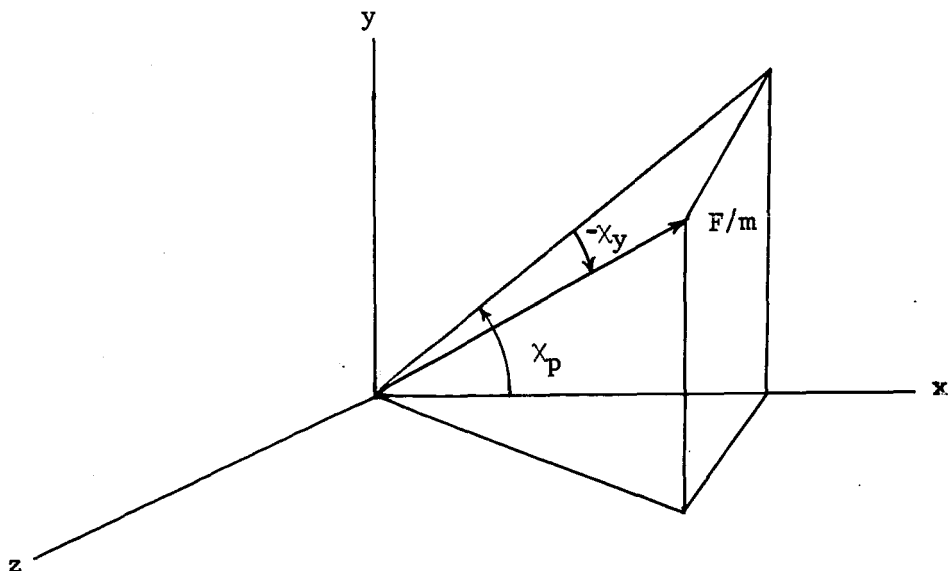
To rotate the direction cosines of the guidance coordinate system to an earth-centered plumbline coordinate system, the inverse of the K matrix is used. This is the system required in the flight computer.

Note that although the guidance scheme computes chi yaw before chi pitch, the rotation order is chi pitch then chi yaw, which is the same as the vehicle platform.

$$\begin{bmatrix} DCX \\ DCY \\ DCZ \end{bmatrix} = \begin{bmatrix} \cos \chi_p & \cos \chi_y \\ \sin \chi_p & \cos \chi_y \\ -\sin \chi_y \end{bmatrix} = \begin{bmatrix} K \end{bmatrix}^{-1} \begin{bmatrix} \cos \chi'_p & \cos \chi'_y \\ \sin \chi'_p & \cos \chi'_y \\ \sin \chi'_y \end{bmatrix}$$

$$\chi_p = \arctan \left(\frac{DCY}{DCX} \right)$$

$$\chi_y = \arcsin (DCZ).$$



B. A Description of the Iterative Guidance Scheme

Some of the basic principles of the iterative scheme can best be demonstrated by assuming constant gravity, thrust and specific impulse. If only a velocity end condition is enforced, it can be shown that a constant thrust direction is the optimum steering law [1]. The thrust direction can be found by the following geometric construction.

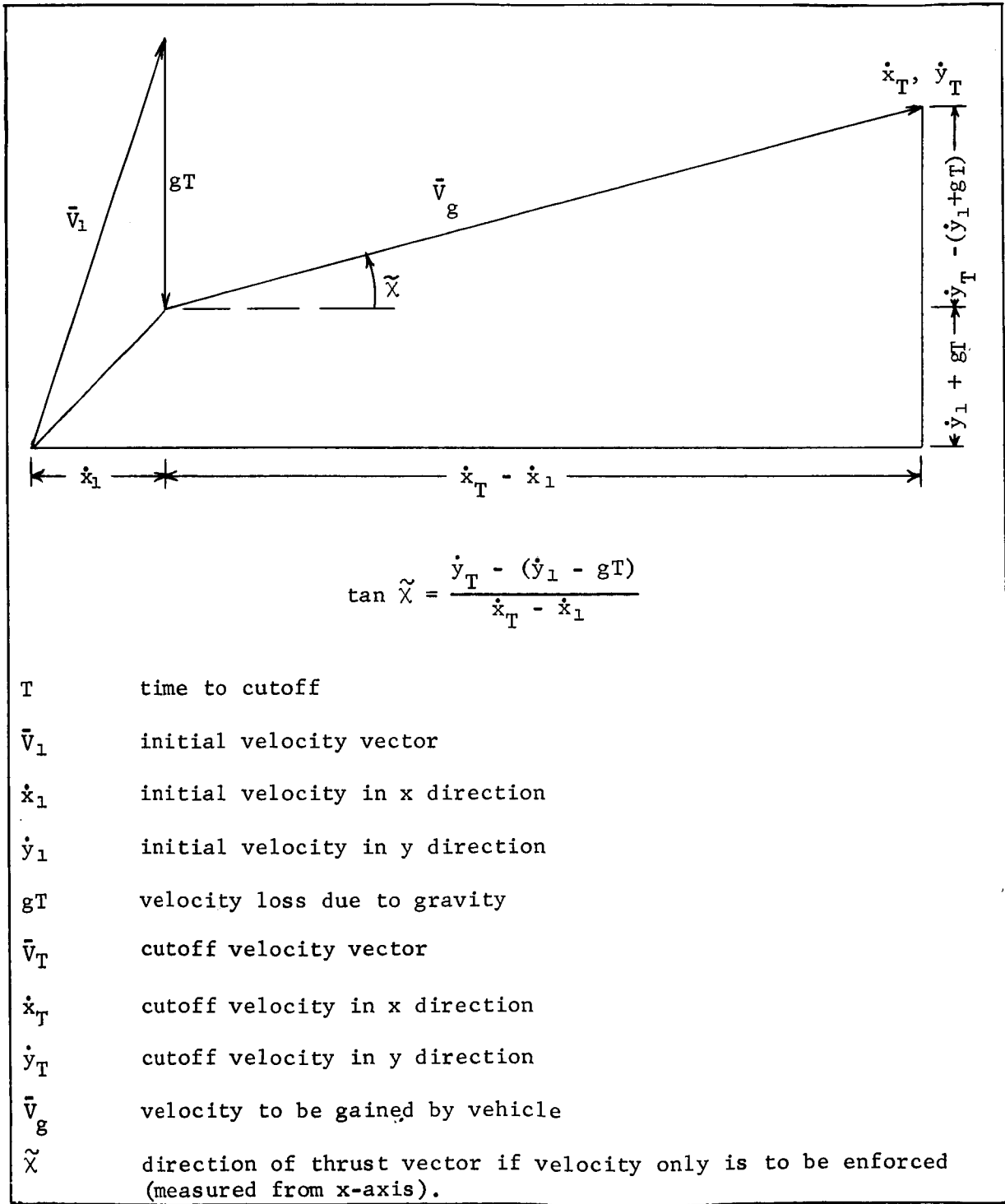


FIGURE 1. THRUST DIRECTION GEOMETRY

If the remaining time, T^* , is not known, it can be estimated by the characteristic velocity equation and updated for each guidance evaluation cycle. Terminal velocity components \dot{x}_T and \dot{y}_T are assumed constants. As time-to-burn approaches zero (cutoff), the steering commands are frozen to avoid indeterminate expressions. Since actual vehicle implementation procedures require frozen steering functions near cutoff, no scheme generality is sacrificed.

A constant thrust direction cannot enforce both altitude and velocity. Therefore, a different steering law is needed. The steering law which the iterative uses is

$$\chi = \tilde{\chi} - K_1 + K_2 \delta t,$$

where K_1 and K_2 are subject to the conditions that the velocity constraint enforced by $\tilde{\chi}$ is not violated. Each evaluation cycle updates $\tilde{\chi}$, K_1 and K_2 using the current state variables and vehicle characteristics. Small δt is the time since the last guidance evaluation cycle.

This new steering law has a theoretical basis: the first order expansion of the calculus of variations steering law derived subject to the same assumptions (flat earth, constant thrust and specific impulse, altitude and velocity enforced, no range enforcement) is

$$\chi = a + bt$$

where a and b are computed subject to current state variables, vehicle characteristics and desired terminal conditions.

It is possible to avoid specifying lateral terminal displacement and velocity components. This is accomplished by defining a guidance reference coordinate system that has one axis perpendicular to the final cutoff plane (Figure 2). All calculations by the guidance equations are done in the guidance reference coordinate system. The coordinates are defined as follows: η is measured from the center of the earth and passes through the final cutoff point, ξ is measured from the center of the earth, perpendicular to η , in the direction of flight, and ζ completes a right-handed coordinate system.

Usually, cutoff conditions are specified as a desired radius (r), velocity magnitude (v), and path angle (θ), measured from the local horizontal. These cutoff conditions transformed to the ξ , η , ζ system are

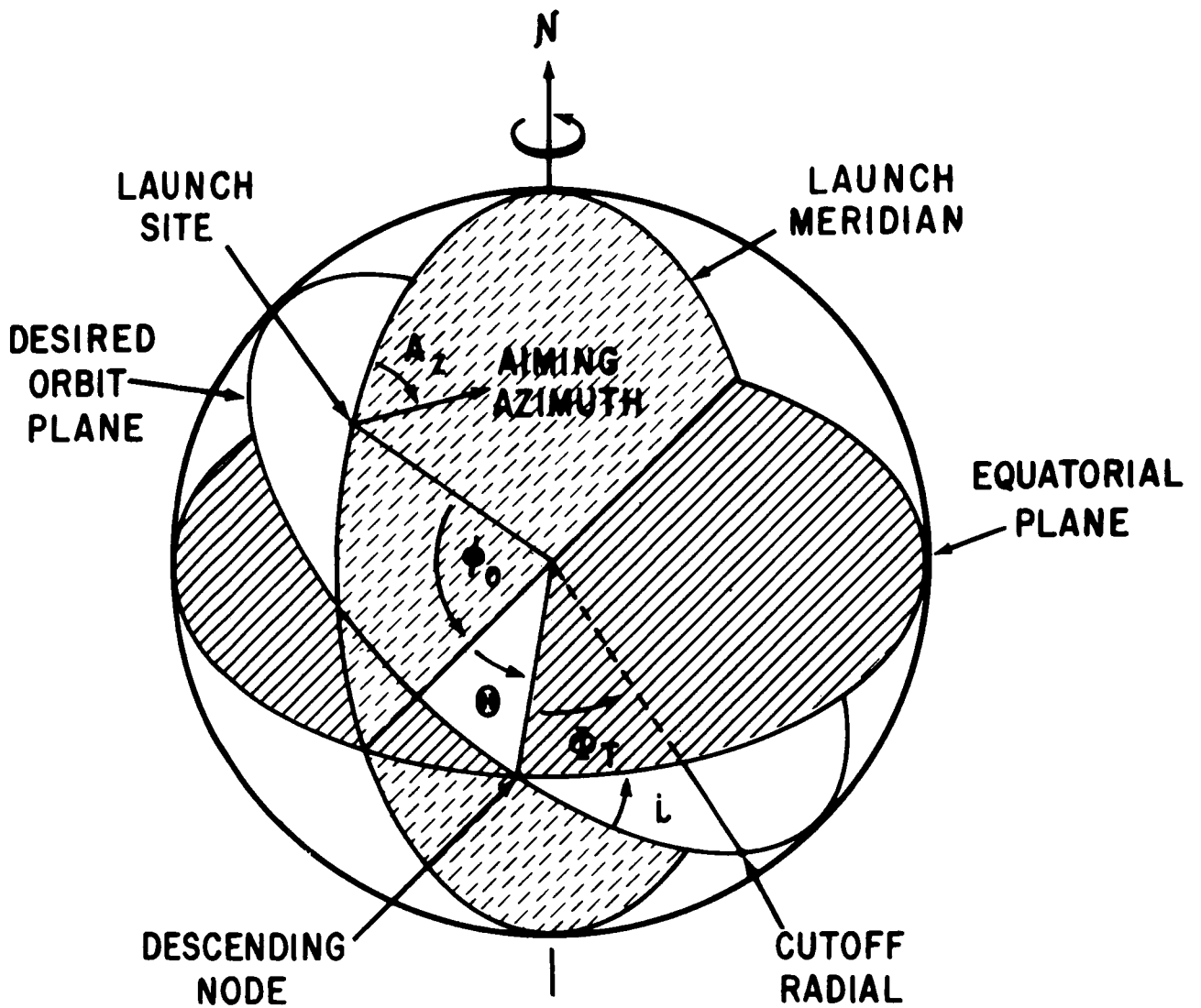


FIGURE 2. GEOMETRY OF GUIDANCE REFERENCE SYSTEM

$$\begin{aligned} \xi_T &= 0 & \dot{\xi}_T &= v \cos \theta \\ \eta_T &= r & \dot{\eta}_T &= v \sin \theta \\ \zeta_T &= 0 & \dot{\zeta}_T &= 0. \end{aligned}$$

To rotate platform coordinates to the desired cutoff plane, the G matrix is computed by the launch vehicle computer. This matrix is a constant and can be computed as soon as launch azimuth, launch latitude, descending node and inclination of the cutoff plane are known. The terminal range angle, ϕ_T , is the remaining rotation necessary to transform from the cutoff plane to the guidance reference system. The matrix that rotates the platform coordinates into the guidance reference system is called the K matrix. It is computed in the coordinate rotation section. The K matrix is updated through ϕ_T every evaluation cycle so that η always passes through the predicted cutoff point. Notice that the predicted terminal values are in the guidance reference system so that ζ_T and $\dot{\zeta}_T$ are zero (ξ_T is zero also).

Time-to-burn is updated based on velocities to be gained measured in the guidance reference system. Cutoff occurs when the vehicle reaches the desired energy. At this time the altitude and path angle constraints will be enforced.

APPENDIX III

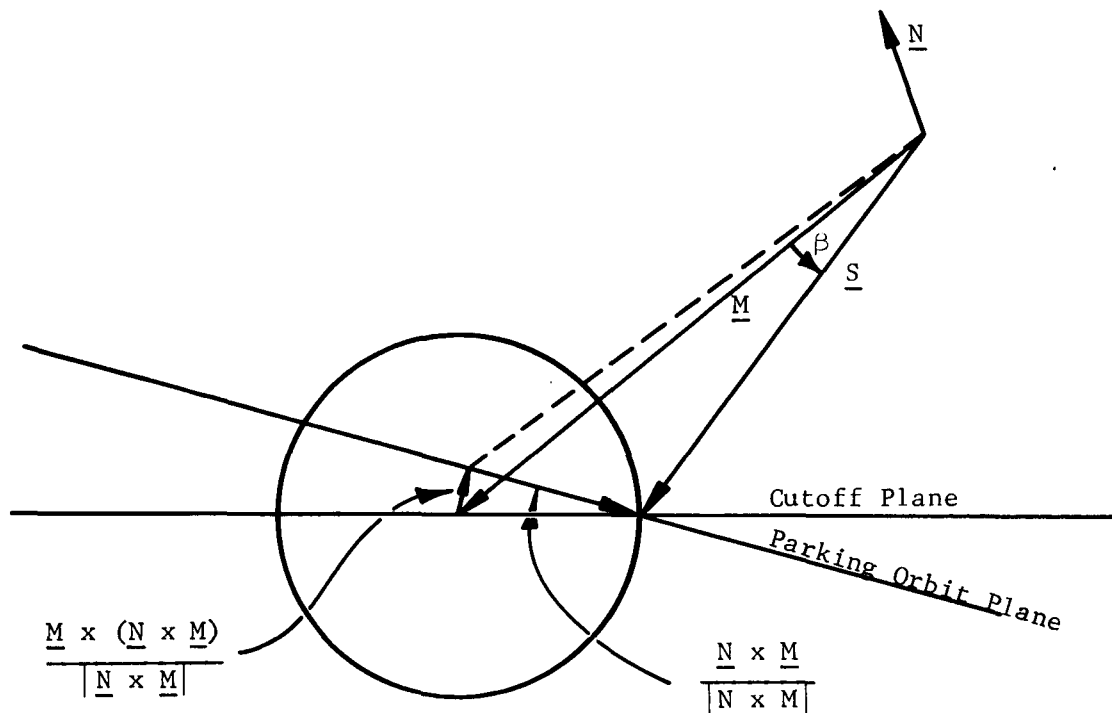
Derivation of the Cutoff Hypersurface Perigee Equation

It has been empirically shown [14] that the injection points of earth-moon trajectories with constant transit times map concentric circles on the surface of the earth. The diameter of these injection rings is a function of the injection path angle. All nominal optimized trajectories generated for a particular vehicle from a circular parking orbit will have almost equal injection path angles. The major lack of path angle uniformity is caused by earth gravitational variations resulting from different launch azimuths. Therefore, the injection ring can be considered to have a constant diameter for the type of trajectories considered in this report.

Each injection point defines a transfer ellipse. The perigee points of these transfer ellipses map a perigee circle which is smaller and concentric to the injection circle. For convenience of representation, the cutoff hypersurface equations are derived based on the perigee ring.

Consider one particular optimum transfer trajectory where an aim point has been selected and the unit aim vector computed as described in Appendix I. A rotation of the trajectory plane about the aim vector will cause the perigee vector corresponding to the transfer ellipse to sweep out a right circular cone. The apex of this cone is the center of the earth and the perimeter of the base is the perigee ring. Notice also that the axis coincides with the unit aim vector.

Since all optimum nominal cutoff planes contain the axis of the perigee cone, the cutoff plane for all earth-moon trajectories is defined to be the plane that contains a perigee vector in the parking orbit plane and the aim vector. The perigee vector in the parking orbit plane will be the vector from the center of the earth to the point of intersection of the parking orbit plane and the perigee circle ahead of the ignition point. Actually, both the perigee and aim vectors are considered unit vectors with separate magnitudes.



\underline{M} unit aim vector

\underline{S} unit perigee vector

β angle between \underline{M} and \underline{S}

\underline{N} unit vector normal to parking orbit plane at ignition.

For clarity of derivation, the aim vector is assumed to point to the center of the perigee circle, and the acute angle between \underline{M} and \underline{S} is defined as β . The perigee vector is computed in an orthogonal coordinate system defined in terms of the two unit vectors \underline{N} and \underline{M} . The axis of the coordinate system are

$\underline{\underline{M}}$ unit aim vector

$\frac{\underline{\underline{N}} \times \underline{\underline{M}}}{|\underline{\underline{N}} \times \underline{\underline{M}}|}$ unit vector in the parking orbit plane

$\frac{\underline{\underline{M}} \times (\underline{\underline{N}} \times \underline{\underline{M}})}{|\underline{\underline{N}} \times \underline{\underline{M}}|}$ unit vector completing the right-handed coordinate system

where $\underline{\underline{N}}$ and $\underline{\underline{M}}$ are computed in the earth centered plumbline coordinate system. Since any vector can be expressed as a linear combination of any other three non-coplaner vectors, let

$$\underline{\underline{S}} = a \underline{\underline{M}} + b \frac{\underline{\underline{M}} \times (\underline{\underline{N}} \times \underline{\underline{M}})}{|\underline{\underline{N}} \times \underline{\underline{M}}|} + c \frac{\underline{\underline{N}} \times \underline{\underline{M}}}{|\underline{\underline{N}} \times \underline{\underline{M}}|}$$

where a , b and c are the direction cosines of $\underline{\underline{S}}$ to be determined. By observation

$$a = \cos \beta$$

and

$$b = - \cos \beta \tan \gamma,$$

where γ is defined by

$$\sin \gamma = \underline{\underline{N}} \cdot \underline{\underline{M}}$$

$$\cos \gamma = |\underline{\underline{N}} \times \underline{\underline{M}}|.$$

Now c can be determined by

$$c = \sqrt{1 - a^2 - b^2} = \sqrt{1 - \cos^2 \beta \sec^2 \gamma},$$

or, in terms of β , \underline{N} and \underline{M} ,

$$c = \frac{\sqrt{|\underline{N} \times \underline{M}|^2 - \cos^2 \beta}}{|\underline{N} \times \underline{M}|} .$$

Since

$$\underline{M} \times (\underline{N} \times \underline{M}) = \underline{N} - (\underline{M} \cdot \underline{N}) \underline{M},$$

\underline{S} can be written as

$$\underline{S} = \left(a - b \frac{\underline{M} \cdot \underline{N}}{|\underline{N} \times \underline{M}|} \right) \underline{M} + b \frac{\underline{N}}{|\underline{N} \times \underline{M}|} + c \frac{\underline{N} \times \underline{M}}{|\underline{N} \times \underline{M}|} .$$

Substituting a , b , c , $-\underline{M}$ for \underline{M} and $\beta = \pi - \phi^*$, the equation for \underline{S} becomes

$$\underline{S} = \left[DD \underline{M} - FF \underline{N} + \frac{\underline{N} \times \underline{M}}{|\underline{N} \times \underline{M}|} \sqrt{\frac{1}{\cos^2 \phi^*} - DD} \right] \cos \phi^*$$

where

$$DD = \frac{(\underline{N} \cdot \underline{M})^2}{|\underline{N} \times \underline{M}|^2} + 1$$

$$FF = \frac{\underline{N} \cdot \underline{M}}{|\underline{N} \times \underline{M}|^2} .$$

This is the form of the perigee vector used in the precompute section on page 16.

A unit vector normal to the cutoff plane can be written as

$$\frac{\underline{S} \times \underline{M}}{\sin \phi^*}$$

Using the normal to the desired cutoff plane, the inclination and descending node can be computed. Next the location of the perigee vector with respect to the guidance reference coordinate system is computed. The cutoff path angle, radius and velocity are computed as functions of true anomaly of cutoff, which is updated every guidance equation cycle by the guidance scheme.

REFERENCES

1. Fried, B. D., "On the Powered Flight Trajectory of an Earth Satellite," Jet Propulsion, Vol. 27, June 1957, pp. 641-643.
2. Lawden, D. F., "Optimal Rocket Trajectories," Jet Propulsion, Vol. 27, December 1957, p. 1263.
3. Smith, Isaac E., and Emsley T. Deaton, Jr., "An Iterative Guidance Scheme for Ascent to Orbit (Suborbital Start of the Third Stage)," MSFC Technical Paper MTP-AERO-63-44, Huntsville, Alabama, 1963, Unclassified.
4. Horn, Helmut J., Daniel T. Martin and Doris C. Chandler, "An Iterative Guidance Scheme and its Application to Lunar Landing," MSFC Technical Paper MTP-AERO-63-11, Huntsville, Alabama, 1963, Unclassified.
5. Martin, Daniel T. and H. L. Hooper, "A Simplified Cutoff Hypersurface for Iterative Guidance During the Lunar Injection Burn," NASA TM X-53025, March 17, 1964.
6. Smith, Isaac E., and F. Don Cooper, "Launch Vehicle Guidance Equations for the Saturn IB SA-202 Mission," NASA TM X-53266, May 24, 1965, Unclassified.
7. Smith, Isaac E., "A Three Dimensional Ascending Iterative Guidance Mode," NASA TM X-53258, May 12, 1965, Unclassified.
8. Cooper, F. Don, "A Computer Program Implementing the Saturn V Guidance Equations for Near-Earth and Lunar Missions," MSFC, Aero-Astroynamics Internal Note #13-65, May 14, 1965, Unclassified.
9. Tucker, W. B., "Lunar Flight Study Series, Volume 7: Principles for Reducing Earth-Moon Trajectory Analysis to Fundamentals," MTP-AERO-63-25, April 16, 1963.
10. Kizner, W., A Method of Describing Miss Distances for Lunar And Interplanetary Trajectories, Ballistic Missile and Space Technology, Vol. III, 1961.
11. Miner, W. E. and Silber, R., "Launch Window Studies Employing Variational Calculus to Determine Optimum Three-Dimensional Trajectories Leading to Injection into a Space Fixed Circular Orbit," American Rocket Society 17th Annual Meeting, November 1962.
12. Holdrige, D. B., "Space Trajectories Program for the IBM 7090 Computer," Jet Propulsion Laboratory Technical Report #32-223, March 1962.

REFERENCES (Continued)

13. Tucker, William B., "Some Efficient Computation Techniques Including their Application to Time Optimal Trajectories from Parking Orbit," NASA Technical Note TN D-2691, March 1965, Unclassified.
14. Braud, Nolan J., "Lunar Flight Studies: Volume 4, Preliminary Investigation of the Astronautics of Earth-Moon Transits," MSFC Technical Paper, MTP-AERO-63-7, January 28, 1963, Unclassified.
15. Clarke, Victor C., Jr., "Design of Lunar and Interplanetary Ascent Trajectories," Jet Propulsion Laboratory Technical Report #32-30, July 26, 1960, Unclassified.
16. Kaplan, Wilfred, Advanced Calculus, Addison-Wesley Publishing Co., Reading, Massachusetts, 1957.
17. Hay, G. E., Vector and Tensor Analysis, Dover Publications, Inc., New York.
18. Cooper, F. Don, "Implementation of the Saturn V Guidance Equations for Lunar Missions from an Earth Parking Orbit," Presented at the Twelfth Flight Mechanics, Dynamics, Guidance and Control Panel Meeting, Manned Spacecraft Center, Houston, Texas, April 14, 1965, Unclassified.
19. Braud, Nolan J., "Lunar Flight Study Series: Volume 3, Earth to Moon Trajectory Investigation for Mission Profiles Involving a Lunar Parking Orbit," MSFC Technical Paper MTP-AERO-62-84, November 15, 1962, Unclassified.
20. McDaniel, Gary, "A Survey of the Influence of Variations in Stage Characteristics on Optimized Trajectory Shaping, Part II: Transfer from Circular Orbits into a Space Fixed Ellipse," MSFC Technical Paper MTP-AERO-63-38, May 20, 1963, Unclassified.
21. Kalensher, B. E., "Selenographic Coordinates," Jet Propulsion Laboratory Technical Report #32-41, February 24, 1961, Unclassified.

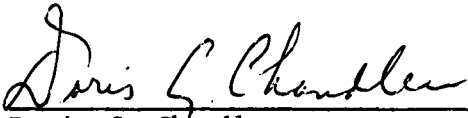
APPROVAL

TM X-53268

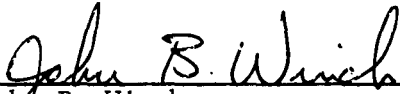
A METHOD OF IMPLEMENTING CUTOFF CONDITIONS FOR SATURN V LUNAR MISSIONS
OUT OF EARTH PARKING ORBIT ASSUMING A CONTINUOUS GROUND LAUNCH WINDOW

By F. Don Cooper

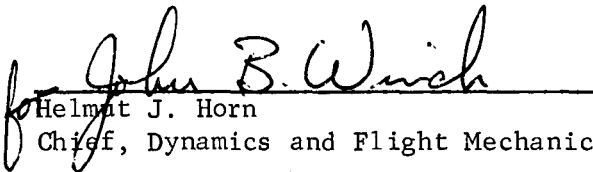
The information in this report has been reviewed for security classification. Review of any information concerning Department of Defense or Atomic Energy Commission programs has been made by the MSFC Security Classification Officer. This report, in its entirety, has been determined to be unclassified.



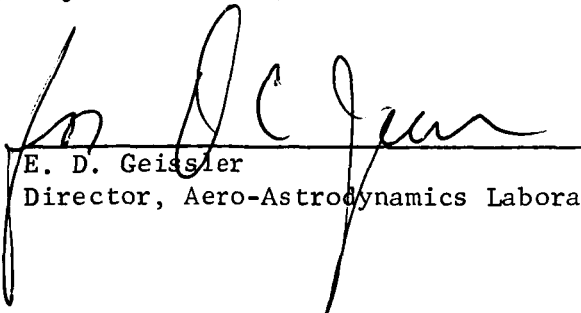
Doris C. Chandler
Chief, Guidance Applications Section



John B. Winch
Acting Chief, Applied Guidance & Flight Mechanics Branch



Helmut J. Horn
Chief, Dynamics and Flight Mechanics Division



E. D. Geissler
Director, Aero-Astrodynamic Laboratory

DISTRIBUTION

DIR

DEP-T

R-DEP-DIR

R-SA

Mr. Dannenberg

I-I/IB-DIR

Col. James

I-I/IB-E

Mr. Vruels

I-DIR

Col. O'Conner

I-IB/V-CE

Dr. Mrazek

I-I/IB-E

Mr. Callaway

R-SA

Dr. J. Kuettner

MS-IP

MS-IL (8)

CC-P

I-RM-M

MS-H

MS-T (5)

Roy Bland

R-ASTR

Dr. Haeussermann
Mr. Brandner
Mr. Hosenthien
Mr. Moore
Mr. Richards

R-ASTR

Mr. Scofield
Mr. Brooks
Mr. Wood
Mr. Blackstone
Mr. Chubb
Mr. Mack
Mr. Brown (3)

R-P&VE

Mr. Cline
Mr. Black

R-AERO

Dr. Geissler
Mr. Dahm
Mr. W. Vaughan
Mr. Baker
Mr. Ryan
Mr. Wittenstein
Mr. Buckelew
Mr. Rheinfurth
Mr. Horn
Mr. Winch
Mr. Cremin
Mrs. Chandler (2)
Mr. I. E. Smith (4)
Mr. McNair (8)
Mr. Ledford
Mr. Stone
Dr. Speer (3)
Mr. Teague
Mr. Kurtz
Mr. Lindberg
Mr. Hardage
Mr. Donehoo
Mr. Cummings
Mr. Dalton
Mr. Scoggins
Mr. Lifsey
Mr. Thomae
Mr. Lovingood
Mr. Mowery
Mr. Hart
Mr. Weiler
Mr. Graham
Mr. Goldsby

DISTRIBUTION (Continued)

R-AERO (Continued)

Mrs. Bauer
Mr. Watkins
Mr. Burrows
Mr. McDaniel
Mr. Lester
Mrs. Brandon
Mr. Telfer
Mr. A. W. Deaton (50)

Scientific and Technical Information Facility (25)
Attn: NASA Representative (S-AK/RKT)
P. O. Box 5700
Bethesda, Maryland

EXTERNAL DISTRIBUTION

Space Technology Laboratories
6001 Gulf Freeway
Houston, Texas
Attn: Mr. C. V. Stableford
Mr. F. D. Cooper (10)

Massachusetts Institute of Technology
Instrumentation Laboratory
68 Albany St.
Cambridge, Mass. 02139
Attn: Mr. John Dahlen
Mr. Michael Richter
Mr. Ed Copps

The Boeing Company
Huntsville, Alabama
Attn: Mr. Wes Morgan
Mr. Dan Martin

Northrop Corporation
Huntsville, Alabama
Attn: Dr. S. Hu
Mr. D. Cooper
Mr. B. Kieth (5)
Mr. R. Kessman

DISTRIBUTION (Cont'd)

Manned Spacecraft Center
Houston, Texas

Attn: Mr. D. B. Pendley
Mr. Shepard
Mr. North
Mr. Woodling
Mr. Duncan
Mr. D. C. Cheatham
Mr. Chambers
Mr. C. Edmiston
Mr. Kotanchik
Mr. St. Legèr
Mr. Wade
Mr. Erb
Mr. Eggleston
Mr. Jackson
Mr. Silveira
Mr. G. S. Lunney
Mr. Thompson
Mr. Huss
Mr. John P. Mayer
Mr. J. A. McAnulty
Mr. H. D. Beck
Mr. R. E. McAdams
Mr. Claiborne R. Hicks, Jr.
Mr. Richard D. Nelson
Mr. Clements
Mr. J. C. Moser
Mr. L. M. Jenkins
Mr. Lanzkron
Mr. R. V. Battey
Mr. O. G. Morris
Mr. Maynard
Mr. Aaron Cohen
Mr. Calvin H. Perrine, Jr.
Mr. Robert J. Ward
Mr. Loftus
Mr. A. Dennett
Mr. E. Hamblett
Mr. R. E. McKann
Mr. Davidson
Mr. Cassetti (5)
Mr. J. Funk
Mr. T. Gibson
Mr. G. Paules

NASA

Headquarters

Washington, D. C.

Attn: Mr. R. V. Sperry, Bellcomm 1021
Mr. R. Wagner, Bellcomm, 1124
Mr. I. Susson, OMSF/MAO
Mr. G. A. Lemke, OMSF/MAR
Mr. M. Savage, OMSF/MAT
Mr. B. Denicke, OMSF/MB

Chrysler Corporation

MICHOUD

New Orleans, La.

Attn: Mr. R. Ross
Mr. J. Swider
Mr. T. Williams